

CHARGE ASYMMETRY IN $\gamma\gamma \rightarrow \mu^+\mu^- + \text{neutrinos}$ WITH POLARIZED PHOTONS

D. A. ANIPKO^a, M. CANNONI^b, I. F. GINZBURG^a, A. V. PAK^a, O. PANELLA^b

^a Sobolev Institute of Mathematics, Novosibirsk, 630090, Russia,

^b LPNHE, 4 Place Jussieu, 75525 Paris, France

^c INFN, Sezione di Perugia, Via G. Pascoli 1, 06129, Perugia, Italy

The difference in distributions of μ^+ and μ^- in reactions $\gamma\gamma \rightarrow \mu^+\mu^- + \nu\bar{\nu}$ and $\gamma\gamma \rightarrow W^\pm\mu^\mp + \nu(\bar{\nu})$ with polarized photons at $\sqrt{s} > 200$ GeV is a large observable effect which is sensitive to New Physics phenomena.

The Photon Collider¹ option of the next generation linear colliders (LC)² offers the opportunity to study with high precision the physics of gauge bosons. The photons with largest energy will be produced mainly in states with definite helicity $\lambda_i \approx \pm 1$. The Standard Model (SM) cross section of $\gamma\gamma \rightarrow W^+W^-$ process at energies greater than 200 GeV is about 80 pb³ and ensures very high event rates. We study the charge asymmetry (CA) of leptons produced in this process in the SM and make preliminary considerations on how these asymmetries change due to some possible effects of New Physics. In this note we present results of Ref.⁴ and some results obtained after that publication.

■ **Diagrams. Qualitative description.** In SM, at the tree level, the process $\gamma\gamma \rightarrow \mu^+\mu^-\nu\bar{\nu}$ is described by 19 diagrams, subdivided into five classes, shown in Fig. 1. The collection of diagrams within each class is obtained from those shown in the figure with the exchange $+ \leftrightarrow -$, $\nu \leftrightarrow \bar{\nu}$ and permutations of photons. For each class we first give an estimate of its contribution to the total cross section, based on the equations for $2 \rightarrow 2$ processes at $s \gg M_W^2$, assuming for the SM gauge couplings $g^2 \sim g'^2 \sim \alpha$ and denoting $B = Br(W \rightarrow \mu\nu)$ and $B_Z = Br(Z \rightarrow \nu\bar{\nu})$:

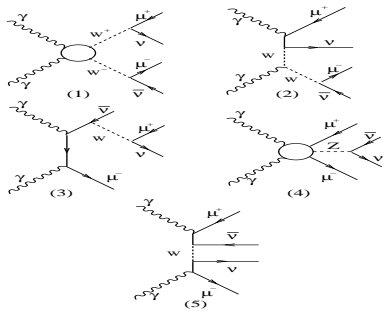


Figure 1: Classes of tree level contributing Feynman diagrams.

(1) 3 double-resonant diagrams (DRD) describe WW production and decay, $\sigma_1 \sim (\alpha^2/M_W^2)B^2 \approx \sigma_{tot}$;

(2) 4 single-resonant diagrams with W exchange in t -channel, $\sigma_2 \sim (\alpha^3/M_W^2)B \sim \alpha\sigma_d/B \sim 0.05 \sigma_{tot}$. This contribution is eliminated almost completely by its interference with DRD;

(3) 4 single resonant diagrams with μ exchange in t -channel (gauge boson bremsstrahlung), $\sigma_3 \sim (\alpha^3/s)B \sim \alpha\sigma_d M_W^2/(Bs) < 0.01\sigma_{tot}$;

(4) 6 diagrams with radiation of Z boson in the process $\gamma\gamma \rightarrow \mu^+\mu^-$, $\sigma_4 \sim (\alpha^3/s)B_Z \sim \alpha\sigma_d M_W^2 B_Z/(B^2s) < 0.01\sigma_{tot}$;

(5) 2 non-resonant diagrams, $\sigma_5 \sim \alpha^4/M_W^2 \sim \alpha^2\sigma_d M_W^2/(B^2s) \ll 0.01\sigma_{tot}$.

The CA is present in the DRD contribution, and simulation shows that the contributions of other diagrams are negligible.

We now give a qualitative discussion of the origin of CA referring to the dominant DRD contribution, $\gamma\gamma \rightarrow W^+W^-$. (i) The cross section practically does not depend on photon polarizations. (ii) The W bosons are distributed around the forward and backward directions³, $d\sigma \propto 1/(p_\perp^2 + M_W^2)^2$. (iii) The helicity of W moving in the positive direction is $\lambda_{W_1} \approx \lambda_1$, while $\lambda_{W_2} \approx \lambda_2$, independently on the charge sign of W (helicity conservation,⁵). (iv) Let the z' -axis be directed along the W momentum \vec{p}_W , $\varepsilon \approx M_W/2$ and $p_{z'}$ the energy and the longitudinal momentum of μ in the W rest frame. The distribution of muons from the decay of W with charge $e = \pm 1$ and helicity $\lambda = \pm 1$ in its rest frame is $\propto (\varepsilon - e\lambda p_{z'})^2$. Hence, the distribution of muons from the decay of W^\pm has a peak along \vec{p}_W if $e\lambda_W = -1$ and opposite to \vec{p}_W when $e\lambda_W = +1$. These distributions are boosted to the $\gamma\gamma$ collision frame. For example, if both colliding photons have $\lambda = -1$, the produced μ^+ are distributed around the upper value of their longitudinal momentum (both in the forward and backward direction), while μ^- are concentrated near the zero value of their longitudinal momentum. This boost makes the distribution in p_\perp wider in the first case and narrower in the second case.

■ **Numerical results** have been obtained with the CompHEP package⁶ considering the complete set of diagrams. The following cuts for background suppression are applied: a cut on the muons scattering angles given by $\pi - \theta_0 > \theta > \theta_0$, with $\theta_0 = 10$ mrad; a cut on muons transverse momentum $p_\perp > 10$ GeV, both on each muon and on the couple of muons. Fig. 2 shows the distributions of muons over longitudinal p_\parallel and transverse p_\perp components of muon momentum $\partial^2\sigma/(\partial p_\parallel \partial p_\perp)$ at different energies for the monochromatic beams. It shows clearly a *strong difference in the distributions of μ^- and μ^+* . The absolute value of the effect decreases with energy due to the increasing importance of the applied cuts. In Fig. 3 we show the same distributions in the form of two-dimensional level lines, for different initial helicity states. Note that the scale of effect in the graphs with μ^- for $(--)$ case differ from other cases by a factor of seven. Due to CP conservation, the μ^\pm distributions for $(--)$ case coincides with μ^\mp distribution for $(++)$ case. The obtained distributions in the (p_\parallel, p_\perp) plane have the form which corresponds to the qualitative picture outlined above.

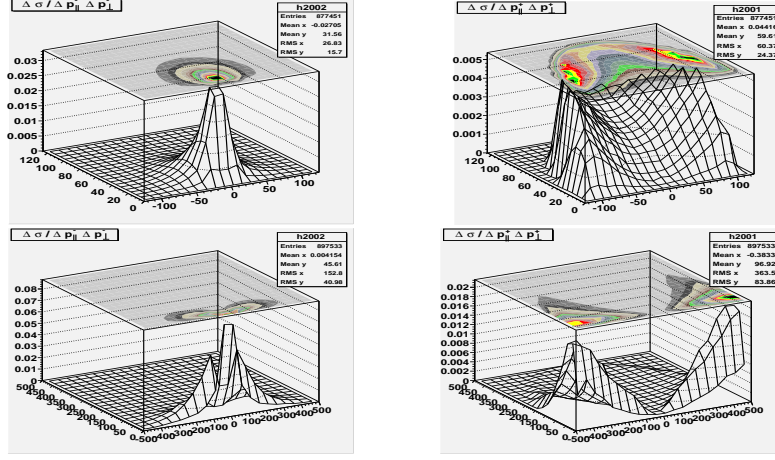


Figure 2: Distributions for $(--)$ helicity of colliding photons: μ^- on the left, μ^+ on the right: $\sqrt{s\gamma\gamma} = 250$ GeV (top) and $\sqrt{s\gamma\gamma} = 1000$ GeV (bottom).

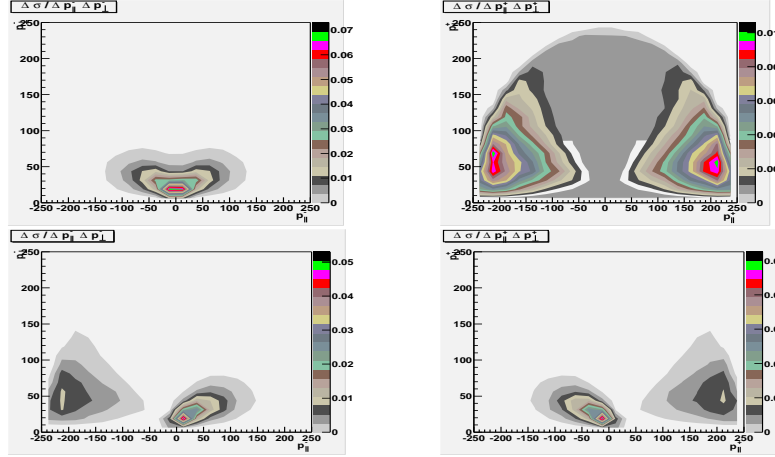


Figure 3: Distributions in the $(p_{\parallel}, p_{\perp})$ plane (pb/bin). Left $-\mu^-$, right $-\mu^+$; helicities of colliding photons: $(--)$ - top, $(-+)$ - bottom, $\sqrt{s\gamma\gamma} = 500$ GeV.

In Ref. ⁴ we also characterized CA by the quantities $\Delta_{L,T} = \frac{P_{L,T+}^- - P_{L,T+}^+}{P_{L,T+}^- + P_{L,T+}^+}$ calculated by the normalized mean values of longitudinal and transverse mo-

mentum of muons flying in the forward hemisphere, $P_{L,T+}^{\pm} = \frac{\int p_{\parallel,\perp}^{\pm} d\sigma}{E_{\gamma max} \int d\sigma}$ and

shown that these quantities change only weakly both using "realistic" photon spectra⁷ and with the addition of the anomalous magnetic moment of W . The quadruple moment of W changes Δ_L significantly at least in the $(- -)$ case: this asymmetry can be useful for the study of the λ anomaly. To mimic the effect of new interactions and/or new particles, we considered a toy model with a "muon" having a mass of 40 GeV. Essential variations are found in this case so that the study of CA can be a useful tool for the discovery of new particles.

■ **Outlook.** The effects considered so far are identical for electrons and muons, thus the same asymmetry will be observed in all $\ell^+\ell^-$ distributions with $\ell = e$ or μ . Therefore, all these contributions should be gathered for a complete analysis. This will enhance the value of the observable cross section for $\gamma\gamma \rightarrow \ell^+\ell^-\nu\bar{\nu}$ from 0.9 pb for to 3.7 pb and for $\gamma\gamma \rightarrow W^+\ell^-\bar{\nu}$, etc. to 23.5 pb (millions of events per year). The observable final state receives contributions also by processes like $\gamma\gamma \rightarrow \mu^+\mu^-\nu\bar{\nu} + \nu\bar{\nu}$ pairs. For example, the most important one will be $\gamma\gamma \rightarrow \tau^+\mu^-\nu\bar{\nu}$, etc., with subsequent decay $\tau \rightarrow \mu\nu\bar{\nu}$. The cross section of this process is 17% of those discussed above ($Br(\tau \rightarrow \mu\nu\bar{\nu}) + 17\%$ for the case with the change $\tau^+ \rightarrow \tau^-$, etc. +3% for $\gamma\gamma \rightarrow \tau^+\tau^-\nu\bar{\nu}$). We plan to consider these qualitatively discussed channels in near future.

This work was supported by grants RFBR 02-02-17884, NSh-2339.2003.2, grant 015.02.01.16 Russian Universities and by the European Union under contract N. HPRM-CT-2002-00311. M. C. thanks "Fondazione Angelo Della Riccia" for a fellowship and C. Carimalo and LPNHE for the kind hospitality.

References

1. I. F. Ginzburg *et al.*, *Nucl. Instrum. Meth.* **205** 47 (1983); *Nucl. Instrum. Meth. A* **219** 5 (1984).
2. B. Badelek *et al.*, "TESLA TDR, p. VI," hep-ex/0108012.
3. I.F. Ginzburg *et al.* *Nucl. Phys.* **B228** 285 (1983).
4. D. A. Anipko *et al.*, *Nucl. Phys. Proc. Suppl.* **126** 354 (2004).
5. M. Baillargeon, G. Belanger, F. Boudjema, hep-ph/9405359.
6. A. Pukhov *et al.*, hep-ph/9908288.
7. I. F. Ginzburg, G .L. Kotkin, *Eur. Phys. J. C* **13** 295 (2000).